1. IGA-BEM 3D lifting flows

as part of

2. the interoperability problem: CAD-SIMulation-shape-OPTimisation

jw: S. Chouliaras, C. Politis, A-A. Ginnis, K. Kostas
S. Khan, M. Diez, A. Serani

Workshop in honor of Professor G.A. Athanassoulis

NTUA, July 4-5, 2022

1. IGA-BEM 3D lifting flows

the problem and its model

velocity potential

- inviscid and icompressible fluid
- irrotational flow in the exterior of the propeller/hub boundaries and an a-priori unknown wake
- moving frame fixed on the propeller blade: $\mathbf{V}_\infty = \mathbf{V}_{in} + \boldsymbol{\Omega} \times \mathbf{r}$
- $\mathbf{V} = \left(\frac{\partial \Phi}{\partial x}, \frac{\partial \Phi}{\partial y}, \frac{\partial \Phi}{\partial z}\right)$
- $\Phi = \phi + \phi_\infty$
  ϕ: perturbation velocity potential
  ϕ_∞: velocity potential at infinity
- $\nabla^2 \Phi = 0$: Laplace field equation

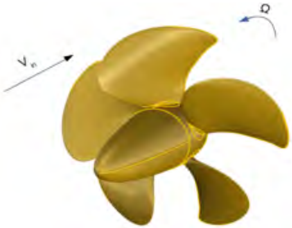

the problem and its model

boundary conditions (bc's)

- kinematic bc on $S_B \cup S_H$:
  $\frac{\partial \phi}{\partial n} = -\mathbf{V}_\infty \cdot \mathbf{n}$
- S_B: blade boundary
- S_H: hub bounsary
- non linear dynamic bc on S_W
- S_W: wake boundary
- $\Delta p = p_u - p_l = 0$, p: pressure
- linear kinematic bc on S_W:
- $\frac{\partial \phi_u}{\partial n} - \frac{\partial \phi_l}{\partial n} = 0$

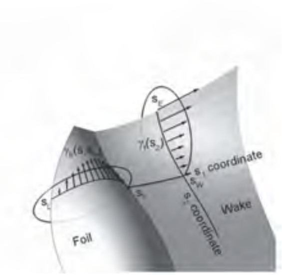

isogeometric boundary element method (IGA-BEM)

- blade S_B and wake S_W will be represented as (bicubic) T-spline surfaces for supporting local refinability
- NURBS (left) knot lines lie on a global rectangular grid
- T-splines (right) can form T-junctions due to locally defined knot vectors
- subject to the condition of: analytical suitability

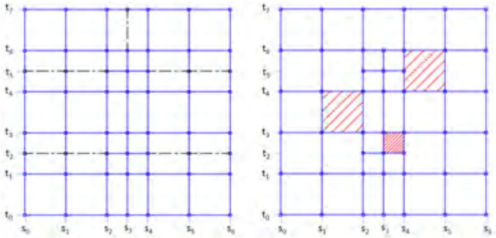

IGA-BEM: parametric plane → manifold

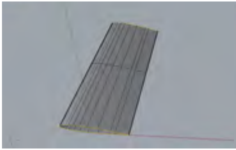

(a) TE DoFs=5

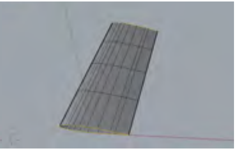

(b) TE DoFs=7

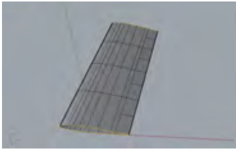

(c) TE DoFs=11

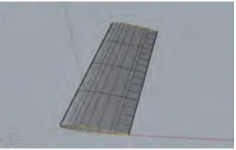

(d) TE DoFs=19

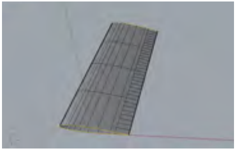

(e) TE DoFs=35

IGA-BEM: boundary integral equation (BIE)

2^{nd} Green's identity & kinematic bc's yield:

$$2\pi\phi(\mathbf{P}) - \int_{S_H+S_B} \phi(\mathbf{Q}) \frac{\partial G(\mathbf{P},\mathbf{Q})}{\partial n} dS - \int_{S_W} \Delta\phi(\mathbf{Q}) \frac{\partial G(\mathbf{P},\mathbf{Q})}{\partial n} dS$$
$$= \int_{S_H \cup S_B} (\mathbf{V}_\infty \cdot \mathbf{n}) G(\mathbf{P},\mathbf{Q}) dS, \quad \mathbf{P} \in S_H \cup S_B \setminus TE,$$

- 3D Laplace basic singularity: $G(\mathbf{P},\mathbf{Q}) = \frac{1}{4\pi} r^{-1}(\mathbf{P},\mathbf{Q})$
- $\phi(\mathbf{P})$: potential on boundary surface
- $\Delta\phi = \phi_u - \phi_l$: potential jump on wake
- $TE = S_B \cap S_W$: propeller's blade trailing edge from which wake emanates

IGA-BEM: employing the isogeometric concept

- the pertubation potential $\phi(\mathbf{P})$ on the blade S_B is projected on the same spline space used for the blade representation
- for the pertubation potential $\phi(\mathbf{P})$ on the wake S_W:
- using Kelvin's theorem we have that $\Delta\phi(\mathbf{P})$ depends only on its trace $\widehat{\Delta\phi}(s_2)$ on TE parametrised wrt s_2
- $\widehat{\Delta\phi}(s_2)$ is projected on the trace of the blade spline space on TE

IGA-BEM: projecting the BIE on the spline space

we get

$$2\pi \sum_{i=1}^{n_B} \phi_i \tilde{R}_i(\mathbf{P}) - \sum_{i=1}^{n_B} \phi_i \sum_{e=1}^{e_B} \int_{S_{B,e}} \tilde{R}_i(\mathbf{Q}) \frac{\partial G(\mathbf{P},\mathbf{Q})}{\partial n(\mathbf{Q})} dS(\mathbf{Q})$$

$$- \sum_{1}^{n_{B,TE}} \widehat{\Delta\phi}_i \int_{S_W} \tilde{R}_i(\xi_{TE},\eta) \frac{\partial G(\mathbf{P},\mathbf{Q})}{\partial n(\mathbf{Q})} dS(\mathbf{Q}) =$$

$$- \sum_{e=1}^{e_B} \int_{S_{B,e}} \mathbf{V}_\infty \cdot \mathbf{n}(\mathbf{Q}) G(\mathbf{P},\mathbf{Q}) dS(\mathbf{Q}), \;\; \mathbf{P} \in S_B \setminus TE$$

- $\tilde{R}_i(\mathbf{Q}(u,v))$: T-spline basis

IGA-BEM: collocating at n_B Greville points

the spline-projected BIE yields n_B equations

$$2\pi \sum_{i=1}^{n_B} \phi_i \tilde{R}_i(\mathbf{P}_j) - \sum_{i=1}^{n_B} \phi_i \sum_{e=1}^{e_B} \int_{S_{B,e}} \tilde{R}_i(\mathbf{Q}) \frac{\partial G(\mathbf{P}_j, \mathbf{Q})}{\partial n(\mathbf{Q})} dS(\mathbf{Q})$$

$$- \sum_{1}^{n_{B,TE}} \widehat{\Delta\phi}_i \int_{S_W} \tilde{R}_i(\xi_{TE}, \eta) \frac{\partial G(\mathbf{P}_j, \mathbf{Q})}{\partial n(\mathbf{Q})} dS(\mathbf{Q}) =$$

$$- \sum_{e=1}^{e_B} \int_{S_{B,e}} \mathbf{V}_\infty \cdot \mathbf{n}(\mathbf{Q}) G(\mathbf{P}_j, \mathbf{Q}) dS(\mathbf{Q}),$$

$$\mathbf{P}_j \in S_B \backslash TE, \quad j = 1, \dots, n_B$$

IGA-BEM: remainig bc's to be satisfied

- zero pressure-jump on the TE: $\Delta p|_{TE} = 0$
- zero pressure-jump on the wake: $\Delta p|_{S_W} = 0$
- **assuming that the wake surface is known** and collocating $\Delta p|_{TE} = 0$ at $n_{B,TE}$ points on TE, we get **a system of quadratic equations with respect to the unknowns** $\Phi = \{\phi_i, i = 1, ..., n_B, \widehat{\Delta\phi}_j, j = 1, ..., n_{B,TE}\}$
- combining the above set with the linear system obtained by collocating the BIE, we get a quadratic system $\mathcal{S}(\Phi) = \mathbf{0}$ of $n_B + n_{B,TE}$ equations for the $n_B + n_{B,TE}$ unknowns Φ
- $\mathcal{S}(\Phi) = \mathbf{0}$ is solved with Newton-Raphson using as starting point the solution of the collocated BIE resulting from applying the Kutta-Morino condition

IGA-BEM: Kutta condition for a NACA 3D wing

pressure near the tip (top) and at the tip (bottom)

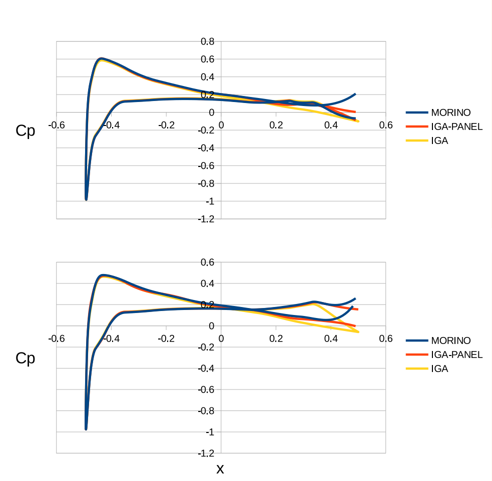

IGA-BEM: next steps

a priori unknown wake surface S_W

- its control points $\mathcal{D}^{\mathcal{W}} = \{\mathbf{d}^{e,W}, e = 1, ..., n_W\}$ should be included in the unknowns
- new set of unknowns: $\Phi \cup \mathcal{D}^{\mathcal{W}}$
- to be determined by adding to the quadratic system $\mathcal{S}(\Phi) = \mathbf{0}$ the zero pressure-jump condition on the wake: $\Delta p|_{S_W}(\Phi \cup \mathcal{D}^{\mathcal{W}}) = 0$

IGA-BEM: next steps

expand the capacity of the basis

- singularities along edges and at vertices:
- wing-tap-intersection: $\nabla\phi = O(r^{-\frac{1}{3}})$
- at the TE-tip: $\nabla\phi = O(r^{-\frac{1}{2}})$

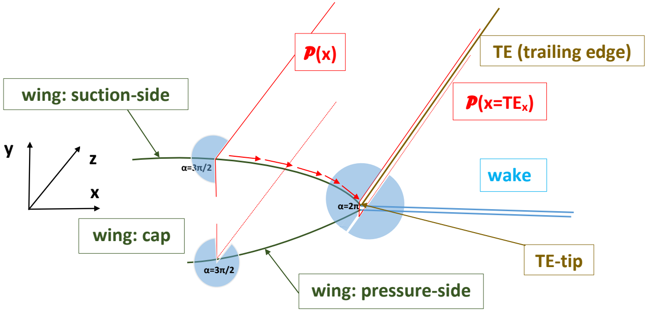

2. The interoperability problem

the workflow in CAD-SIM-OPT loop

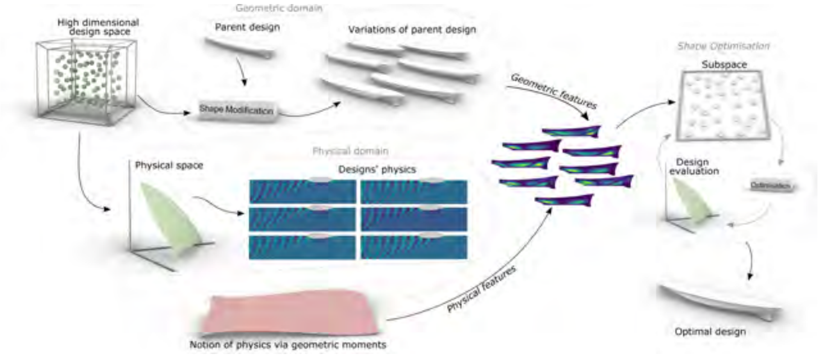

Dimensionality Reduction: literature

- Karhunen-Loève Expansion (KLE)
- Principal Component Analysis (PCA)
- proper orthogonal decomposition and their non-linear extensions, such as
  - kernel PCA
  - LLE (Locally Linear Embedding)
  - ISOMAP
- Machine Learning-based approaches:
  - auto-encoders,
  - Generative-Adversarial Networks (GANs) and variations

literature: limitations

- inability to preserve the shape's complexity and intrinsic underlying geometric structure:
- the resulting subspace lacks the representation *capacity* and *compactness*
- defined as subspace's ability to produce *diverse* and *valid* shapes with least number of latent variables when being explored for shape optimisation
- these deficiencies can hamper the success of the optimiser as it may spend the majority of the available computational budget on exploring infeasible, practically invalid and similar shapes
- the basis of the subspace is solely formulated with geometric features and no information related to physics, against which designs are assessed, is incorporated
- these techniques' inability is also strengthened from the fact that the geometry representations, used in subspace learning, are commonly low-level shape discretisations

our objectives

- a shape-supervised approach, which combines continuous geometry modification with **geometric moments** to harness the compact geometric representation of baseline shape and complement its physics during dimensionality reduction
- therefore, the resulting subspace has not only enhanced representation capacity and compactness to produce a valid and diverse set of design alternatives, respectively, but
- is also physically informed to improve the convergence rate of the shape optimiser towards an optimal solution

literature: about moments

- geometric moments are coupled with physics as they provide the geometric foundation for different physical analyses
- like physics, provide important clues about the distribution of volume and validity of the design
- their evaluation is substantially less expensive
- already used in literature for:
- shape processing tasks such as object recognition
- rigid body transformation
- parametric sensitivity analysis
- material field modelling
- governing equations of motion for flow around a body
- moment-based shape representations are used to aid the interoperability between CAD representations and physics

test case: the DTMB hull model

- The DTMB (David Taylor Model Basin) 5415 hull model is a widely used benchmark ship employed in shape optimisation
- this parent model is considered for the minimisation of the ship hull's wave-making resistance coefficient C_w
- C_w constitutes a considerable part of the ship's total resistance: it corresponds to the energy consumed to generate the free-surface waves

test case: hydrodynamics-moments correlation

- the flow around a slender ship moving on the free surface with a constant velocity can be represented by using an appropriate source-sink distribution along its centre plane
- the strength of these sources is proportional to the longitudinal rate of change of the ship's cross-sectional area and this aspect can be well captured by geometric moments, especially those of higher order
- an early derivation for the evaluation of C_w for slender ships, known as Vosser's integral, reveals explicit dependence on the longitudinal derivative of the cross-sectional area, i.e., $S'(x) = \frac{\mathrm{d}}{\mathrm{d}x}S(x)$ where $S(x) = \int_{\Phi(x)} \mathrm{d}y\mathrm{d}z$ is the cross-sectional area, and $\Phi(x)$ denotes the cross-section of a ship hull at the longitudinal position x.

test case: hydrodynamics-moments correlation

- Let now $m_p = \int_o^L x^p S'(x)\mathrm{d}x$ be the $p-$th order moment of $S'(x)$
- assuming now that $S(0) = S(L) = 0$ we get: which leads to

$$m_p = -pM_{p-1,0,0},$$

where $M_{p-1,0,0}$ is a component of the hull's geometric moments vector of order $s = p + q + r = p - 1$;

- thus, $p-$order 1D moments of $S'(x)$ are directly linked to $(p-1)-$order 3D longitudinal moments of the hull
- thus our design vector is augmented with a physics-informed part expressed by geometric moments

test case: hydrodynamics-moments correlation

- note that one cannot expect that every physical QoI of integral character is strongly connected with the geometric moments of the body
- thus, the usage of moments cannot guarantee a physics-informed subspace
- e.g., viscous-pressure resistance is expressed as an integral over the wetted surface of the body
- nevertheless, it depends on local properties of the surface, such as smoothness and curvature, which can act as turbulence generators by triggering flow separation
- however, even if there is no strong connection of physics under consideration with geometric moments, their usage can still provide a high-level intrinsic geometric information of the shape's geometry, which is imperative to learning an efficient subspace with enhanced representation capacity and compactness.

test case: results

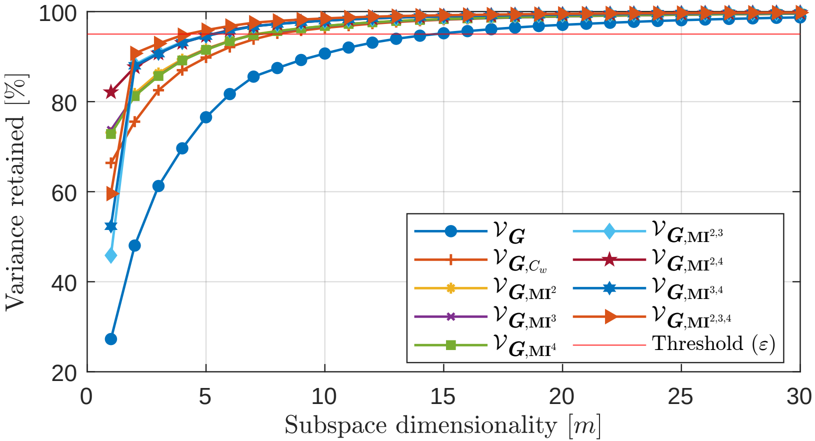

Figure 1: percentage of variance retained by each of the hull model's subspace versus its dimension - the horizontal red line indicates the 95% threshold.

test case: results

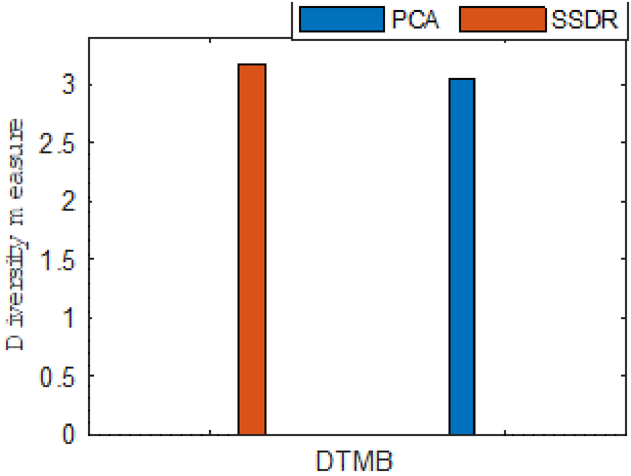

Figure 2: diversity measure: Average of Hausdorff distance between baseline designs and 5,000,000 designs from $\mathcal{V}$

test case: results

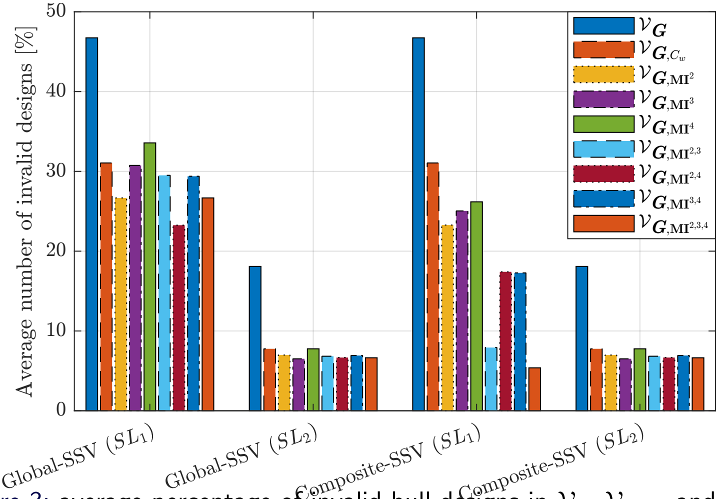

Figure 3: average percentage of invalid hull designs in $\mathcal{V}_{\mathbf{G}}$, $\mathcal{V}_{\mathbf{G},\mathbf{C_w}}$ and shape-supervised subspaces sampling with global- and composite-SSVs when bounded by two different approaches

test case: results

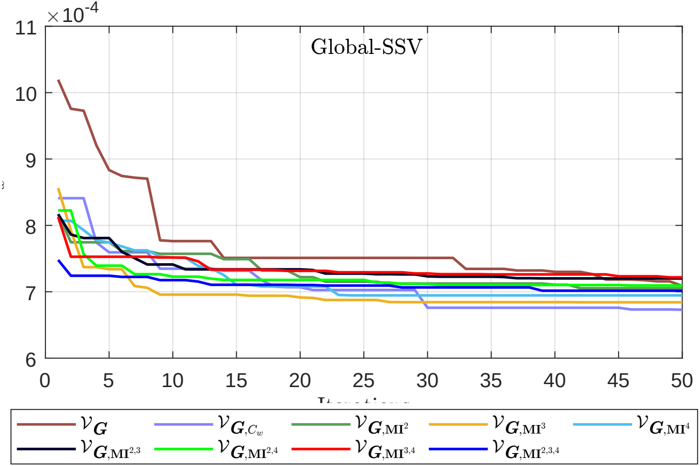

Figure 4: C_w optimisation history for $\mathcal{V}_{\mathbf{G}}$, $\mathcal{V}_{\mathbf{G},\mathbf{C_w}}$, and the shape-supervised subspaces with global-SSV

Any Questions?

Funding:

GRAPES
learninG, pRocessing And oPtimising shapES

European Union's Horizon 2020 research and innovation programme under the Marie Skłodowska-Curie grant.

publications

- S Khan, PK, A Serani, M Diez (2022) **"Geometric moment-dependent global sensitivity analysis without simulation data: application to ship hull form optimisation"**, *Computer-Aided Design*, paper: 103339
- S Khan, PK, A Serani, M Diez, K Kostas (2022) **"Shape-supervised dimension reduction: Extracting geometry and physics associated features with geometric moments"**, *Computer-Aided Design*, paper: 103327
- S Khan, PK (2021) **"From regional sensitivity to intra-sensitivity for parametric analysis of free-form shapes: Application to ship design"**, *Advanced Engineering Informatics*, vol.49, paper: 101314
- SP Chouliaras, PK, KV Kostas, AI Ginnis, CG Politis (2021) **"An Isogeometric Boundary Element Method for 3D lifting flows using T-splines"**, *Computer Methods in Applied Mechanics and Engineering*, vol.373, paper: 113556